Simulation, implementation and evaluation of a low-cost navigation system for an autonomous vehicle

Vítor Jorge Fabião Mendonça
vitorjmendonca@tecnico.ulisboa.pt

Instituto Superior Técnico, Universidade de Lisboa, Portugal

November 2017

Abstract

Nowadays, the development of autonomous vehicles, for outdoor operation, is an area of extreme importance and intensive research, whereby the development of a navigation system that allows guidance is of paramount importance in this field of study. The majority of navigation systems use *Global Navigation Satellite System* (GNSS) as the only source of information regarding position, velocity and attitude. However the GNSS can't always provide reliable and continuous essential information for an autonomous vehicle. This work is intended as a contribution to filling in this gap, as it takes advantage of the reciprocity that exists between the *Inertial Navigation System* (INS) and GNSS presenting an integration (fusion) algorithm, in a loosely coupled approach, using sensors and low-cost equipment and *Extended Kalman Filter* (EKF), which determines the attitude, position, and speed of the vehicle. For that purpose, a simulator in Simulink was developed, which allowed testing of the solution proposed. The interface with the sensors is accomplished by Arduino and an algorithm was developed to carry out the reading and syncing of inertial sensors and the GNSS receiver. Some methods of characterization and calibration of various sensors are also presented. Finally the navigation algorithm is implemented, in Python, using a Raspberry Pi. It was found through the simulator and field testing, that the system responded as predicted on the attitude solution. As far as position is concerned, the algorithm presented a consistent solution, despite some deviations.
Keywords: GNSS/INS Integration, loosely coupled, data fusion, Kalman filters

1. Introduction

Currently, research on intelligent vehicles has been focused on developing vehicles that perform completely autonomous navigation or can partially automate functions of the vehicle in order to improve safety, comfort and performance.

Broadly speaking, an autonomous vehicle must have the ability to "sense" and "model" the environment, determine its location and orientation in space, carry out path planning (mission), make decisions and control its movement with precision, all this in real time in an unknown, highly dynamic environment.

The development of a navigation system that allows guidance, is therefore a relevant part of the problem in this field of study.

Nowadays, most navigation systems use *Global Navigation Satellite System* (GNSS) receivers, namely *Global Positioning System* (GPS), as the only source of information regarding speed, position and attitude [6]. GNSS can provide reliable information about navigation only under ideal conditions, i.e., open spaces, having its performance degraded when the vehicle navigates in urban environments or in areas where it is susceptible to signal blockage from satellites.

More sophisticated applications, such as autonomous vehicles, need to have continuous and reliable navigation information, which means that the GNSS, as a stand-alone system, cannot be used because it does not ensure reliability and it is not always available [6, 8].

An alternative to GNSS is the *Inertial Navigation System* (INS) which uses inertial sensors to provide a navigation solution via dead reckoning. With the development of *Microelectromechanical systems* (MEMS), the price and the size of the inertial sensors have been falling, making them more attractive for the development of navigation systems. INS, given its high frequency of operation, has virtually continuous behaviour, however the performance of inertial sensors degrades, in extended periods of time, due to noise and other sources of error that cause drift in determining the solution of navigation. The reciprocity between the GNSS and the INS, Table 1, makes the fusion (integra-

tion) between the two systems a more robust navigation solution, taking advantage of the benefits of each navigation system, compensating for shortfalls [1, 3, 5, 6, 7].

	GNSS	INS
Localization	Absolute	Relative
Acquisition Frequency	Low	High
Accuracy Short Term	Medium	High
Accuracy Long Term	High	Low

Table 1: Qualitative comparison between GNSS and INS (adapted from [4]).

This study deals with the development of a modular, simple and low cost navigation system, with the objective of implementing it in an autonomous vehicle, that operates outdoors, with the constraints of working in real time. The navigation system must perform the fusion between GNSS and the INS based on MEMS.

In order to solve the data fusion problem it is usual to use *Extended Kalman Filter* (EKF) [3].

Fusion algorithms, based on EKF, are different from each other in that the sensors and models used - error model or total state model - as well by the integration level - loosely coupled or tightly coupled integration - [1, 7].

In this paper a loosely coupled total state fusion algorithm it will be developed, making some improvements to the paper from [2].

2. Background

2.1. Inertial Navigation System (INS)

An INS is composed of an *Inertial Measurement Unit* (IMU) which contains three orthogonal rate-gyroscopes and three orthogonal accelerometers, measuring angular velocity and linear acceleration, respectively. MEMS based IMU makes use of a *strapdown algorithm* to provide a navigation solution, shown in Figure 1.

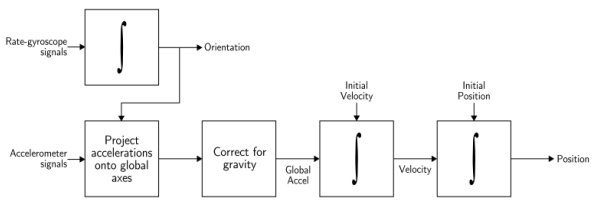

Figure 1: Strapdown inertial navigation algorithm [10].

MEMS-based IMU estimate the attitude, in three dimensional motion, of a vehicle from the integration of the angular rates about the body axes x, y, z denoted ω_{x_b}, ω_{y_b}, ω_{z_b} measured from rate gyros. The relationship between body rates and Euler angle rates is given by [9]:

$$\begin{bmatrix} \dot{\phi} \\ \dot{\theta} \\ \dot{\psi} \end{bmatrix} = \begin{bmatrix} 1 & \sin\phi\tan\theta & \cos\phi\tan\theta \\ 0 & \cos\phi & -\sin\phi \\ 0 & \dfrac{\sin\phi}{\cos\theta} & \dfrac{\cos\phi}{\cos\theta} \end{bmatrix} \begin{bmatrix} \omega_{x_b} \\ \omega_{y_b} \\ \omega_{z_b} \end{bmatrix} \quad (1)$$

where:

- ϕ: roll angle;
- θ: pitch angle;
- ψ: yaw angle.

The accelerometers measure specific force about each body axis:

$$\boldsymbol{f_b} = \begin{bmatrix} f_{x_b} \\ f_{y_b} \\ f_{z_b} \end{bmatrix} = \boldsymbol{a_b} - \boldsymbol{g_b} \quad (2)$$

where $\boldsymbol{a_b}$ is the vector of the acceleration sensed by the body and $\boldsymbol{g_b}$ is the gravity vector in body coordinates. The velocity and position of the vehicle is obtained in the *North East Down* (NED) reference system according to Figure 1.

2.2. Magnetometers

MEMS-based magnetometers measure the strength of the earth's magnetic field, in body axes m_{x_b}, m_{y_b}, m_{z_b}.

Magnetometer can be used to estimate magnetic heading (ψ_{mag}) [3]:

$$\psi_{mag} = \text{atan2}\left(\frac{m_{z_b}\sin\phi - m_{y_b}\cos\phi}{m_{x_b}\cos\theta + m_{y_b}\sin\phi\sin\theta + m_{z_b}\cos\phi\sin\theta}\right) \quad (3)$$

ψ_{mag} can be used to estimate the vehicle yaw angle, ψ.

2.3. Global Positioning System (GPS)

GPS is used to provide the vehicle position and velocity in global coordinates. A GPS receiver provides latitude, longitude and height above WGS84 ellipsoid as well as the three dimensional velocity in navigation coordinates - NED. After converting latitude, longitude and height to NED, GPS provides the following information:

- $P_{x_{nGPS}}$: North position;
- $P_{y_{nGPS}}$: East position;
- $P_{z_{nGPS}}$: Down position;
- $V_{x_{nGPS}}$: North velocity;
- $V_{y_{nGPS}}$: East velocity;
- $V_{z_{nGPS}}$: Down velocity.

In this study the *European Geostationary Navigation Overlay Service* (EGNOS) was also used, a *Satellite-Based Augmentation System* (SBAS) that not only provides some correction parameters for GPS solution, thus augmenting its precision, but also integrity information.

2.4. GPS/INS Integration

GPS/INS integration algorithm used the EKF formulation described in the master thesis associated with this extended abstract.

The developed filter aims to estimate the vehicle's attitude, as well as its position, and speeds in NED frame. The state vector is given by:

$$\boldsymbol{x} = \begin{bmatrix} \phi & \theta & \psi & P_{x_n} & P_{y_n} & P_{z_n} & V_{x_n} & V_{y_n} & V_{z_n} \end{bmatrix}^T \quad (4)$$

The dynamic model of the filter is given by (A.5). Two models were developed for the observations. The first one, described by (A.6) is used if the GPS is available. The first part of (A.6), $\boldsymbol{m_b} = C_n^b \boldsymbol{m_n}$, represents the rotation of the earth's magnetic field in NED to the body axes reference system. As magnetometers are not sensitive to the vehicles' accelerations, they are an effective way of estimating the vehicles attitude, it is only necessary to know local earth's magnetic field strength which can be found from databases. The drawback of using magnetometers is that they are heavily influenced by local perturbations. In order to solve this issue, a characterization method is presented in this thesis. The second part of (A.6) states that the position and velocities of the vehicle in the NED reference system are directly corrected from GPS observations.

When GPS is not available the second model is used, described by (A.7). The first part of (A.7) was already justified. The second part is concerned with the correction of the position estimate of the vehicle through accelerometers observation.

3. Simulator and Implemented System

As a first step a simulator was developed that aimed, to create, test and validate the navigation system to be implemented, being therefore a key part of this work. This simulator was developed by modules so that it would be possible to replace all simulated components, including all sensors, for real ones.

The MATLAB package Simulink was used to develop the simulator.

The second phase dealt with the implementation of the navigation system with real sensors. First off all, market research was conducted in order to choose and acquire all sensors and equipment needed. The navigation system developed uses an Arduino MEGA to interface with the sensors - Pololu's AltIMU-10 v4 and the SainSmart's Ublox NEO-6M Uart/IIC receiver.

The navigation system developed has two operating modes:

- Offline mode: in this mode *raw data* from Arduino is saved on a micro-SD card, being post-processed in Simulink. This operating mode was used in the tests and results phase.
- Online mode: in this mode *raw data* from Arduino is processed in real-time by a Raspberry Pi which contains the integration algorithm.

Figure 2 shows the schematic with the navigation system developed.

3.1. Arduino

Besides setting up and reading out the sensors, one of the main issues with Arduino was the synchronisation between the GPS receiver which works at 5Hz and the IMU that has a sampling frequency of 50Hz. The problem is that it is necessary to be sure that the data coming from two sensors refers to the same time instant. The only way that makes sense to carry out data fusion is if, and only if, this is accomplished. This issue was solved by putting a time tag on the raw messages that come from Arduino. GPS time was used as time reference. There are ten samples from the IMU between two consecutive GPS samples. To ensure that the IMU data was sampled at 50Hz, a timer interruption routine from Arduino was employed. In Figure 3 it is possible to observe theoretically how the syncing mechanism works.

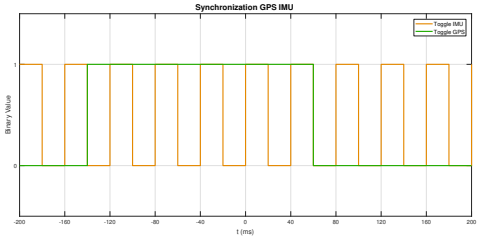

Figure 3: Synchronization GPS IMU - theoretical.

With the help of an oscilloscope it was possible to test the syncing mechanism, the results are given in Figure 4.

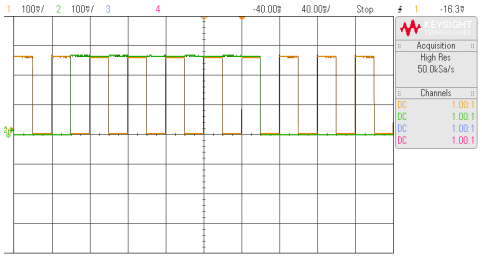

Figure 4: Synchronization GPS IMU - experimental (GPS - green e IMU - orange).

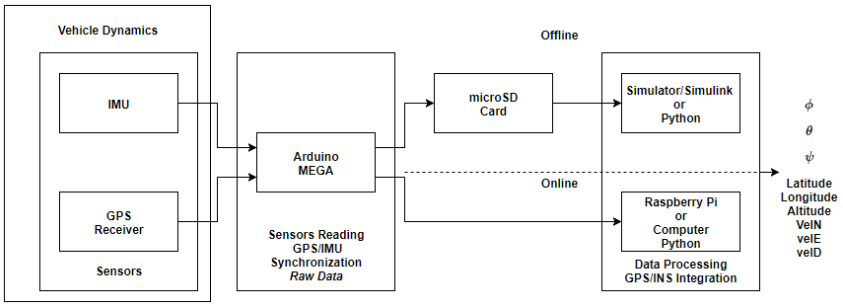

Figure 2: Schematic of the developed navigation system.

Notice that the toggle present on Figure 4 has half the sampling frequency previously defined, this happens because data from GPS and IMU are sampled both on the rising and falling edges.

The results gathered from the oscilloscope were the following:

- GPS
  - Frequency → 2.499Hz
  - Duty Cycle → 50.001%
- IMU
  - Frequency → 24.950Hz
  - Duty Cycle → 50.070%

The results above allow us to conclude that the two sensors are synced.

4. Tests and Results

4.1. Simulator

In the simulator a differential drive car model was implemented which described a circular trajectory with a radius of 9.15m. First of all, the Kalman filter algorithm was tested without GPS signal losses.

The attitude solution can be observed in Figure 5.

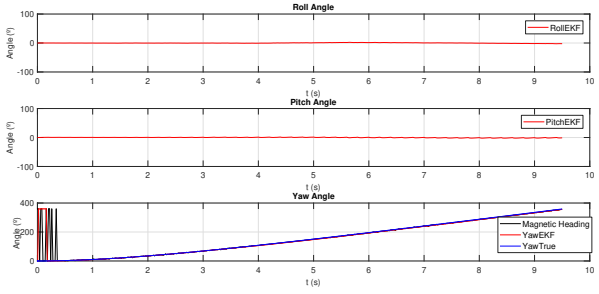

Figure 5: Vehicles' attitude - simulator no GPS signal losses

The graphs in Figure 5 show that the roll and pitch angle behave as expected as the vehicle moves on the horizontal plane. The yaw angle also behaves well as the vehicle is describing a complete circle.

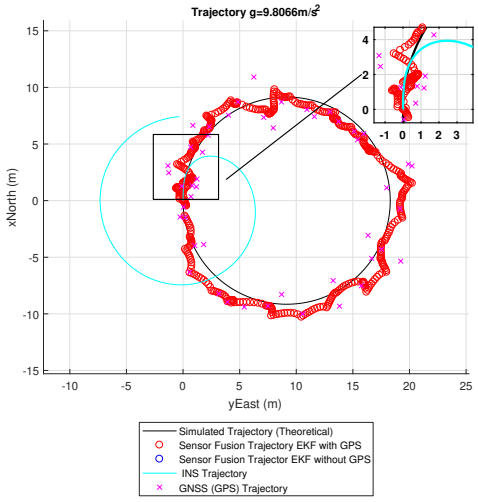

Figure 6: Horizontal plane trajectory - simulator no GPS signal losses.

In Figure 6 it is possible to observe the drift on the INS navigation solution as a stand-alone system (cyan). It is also possible to observe the differences, as far as continuity is concerned, between the GPS solution stand-alone (pink crosses) and the integrated solution (red).

The final output of the navigation system (red) does not differ too much from the reference trajectory (black).

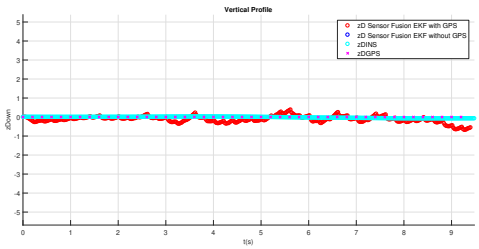

Figure 7: Vertical profile - simulator no GPS signal losses.

It is possible to observe from Figure 7 that the integrated solution presents some deviations from the reference $z_D = 0$.

Simulations were conducted in order to evaluate the system response when there is a GPS signal loss. It was simulated a GPS signal loss between 5s and 7s. The attitude solution is presented in Figure 8.

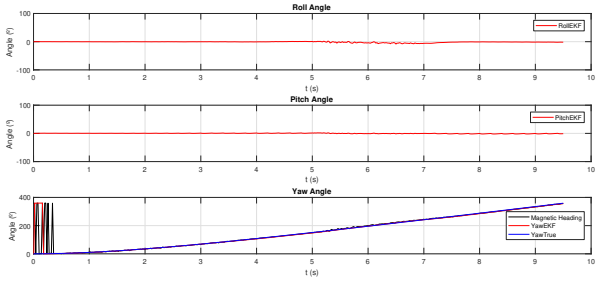

Figure 8: Vehicles' attitude - simulator with GPS signal losses

From Figure 8 it is possible to observe that attitude estimate follows what is expected. Figures 9 and 10 show a detail of what happens to roll and pitch angle during GPS signal loss.

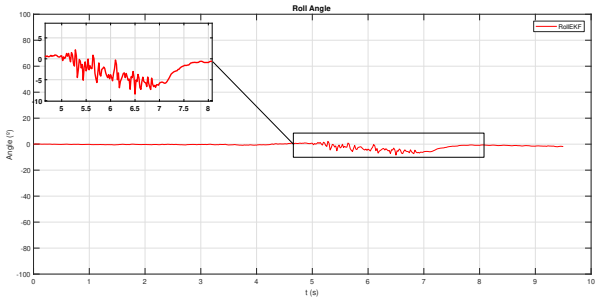

Figure 9: Detail roll angle.

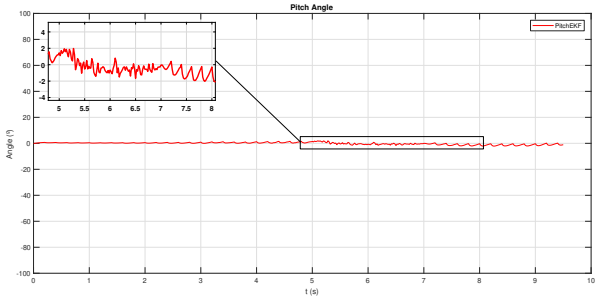

Figure 10: Detail pitch angle.

From Figure 9 it is possible to observe that when there is GPS signal loss, roll angle drops to 8.43° at time instant 6.5s. When GPS becomes available roll angle recovers, stabilizing at −1.37°. With respect to pitch angle it is possible to observe that GPS signal loss does not have a major influence on its estimation.

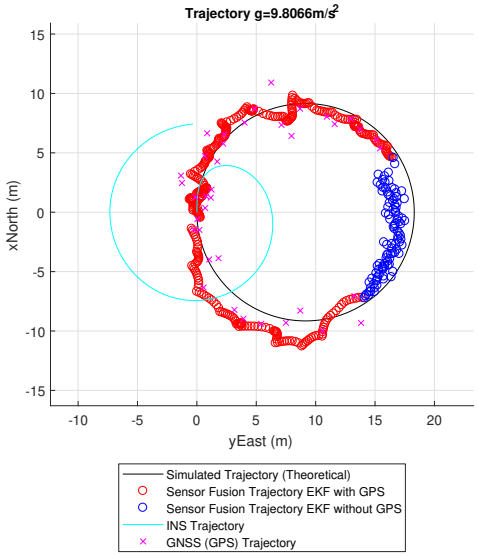

Figure 11: Horizontal plane trajectory - simulator with GPS signal losses.

From Figure 11 it possible to observe (blue) that when there is a GPS signal loss the estimated position solution can follow the curve without a major deviation. It is also possible to observe that there is a high frequency navigation solution.

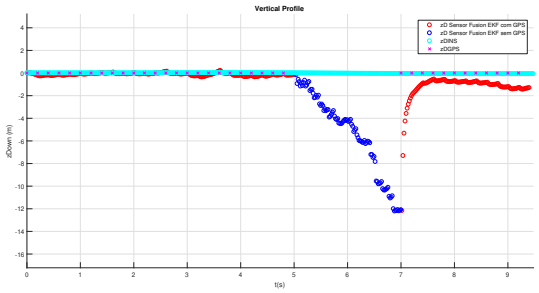

Figure 12: Vertical profile - simulator with GPS signal losses.

In Figure 12 it is possible to observe that when there is a GPS signal loss the navigation solution diverges, reaching a minimum of −12.22m.

4.2. Yaw Angle

An indoor test was conducted with a quasi-static motion, in order to observe the vehicle's attitude estimation, namely the yaw angle estimation. Before starting this test it was not only necessary to calibrate the magnetometers but also perform a gravity acceleration value estimation. The test consisted of rotating the Arduino over a surface with marks indicating the angle of rotation. Initially, with the help of a compass, the Arduino was aligned with the south direction.

The results are shown in Figure 13.

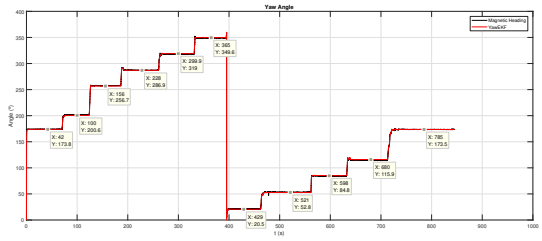

Figure 13: Yaw Angle test.

Results show that yaw angle estimation presents a filtered and fast response. An average error of 1.9° was obtained. The biggest error in this trial was 3.9°.

4.3. Real Path - Car

In order to test the navigation system, in a dynamic and real environment, a car test was carried out. The test consisted of doing three consecutive laps around the circuit shown in Figure 14. This test had the goal of evaluating the system's consistency and precision.

Figure 14: Map: Theoretical circuit.

In Figure 15 it is possible to observe the attitude solution for the three consecutive laps. In this Figure it is possible to notice a pattern on the yaw angle that corresponds to the three laps made, this result reveals consistency in the attitude determination. There is also good precision on attitude estimation as is explained in the master thesis.

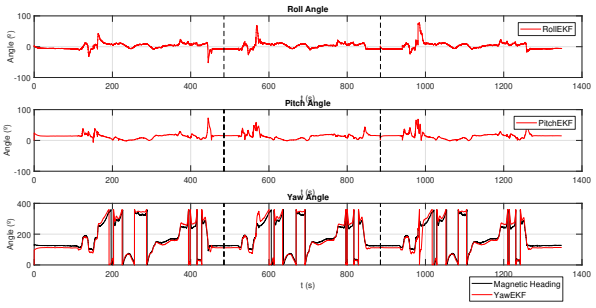

Figure 15: Vehicles' attitude - real path - car.

From Figure 16 it is possible to observe a comparison between the three laps.

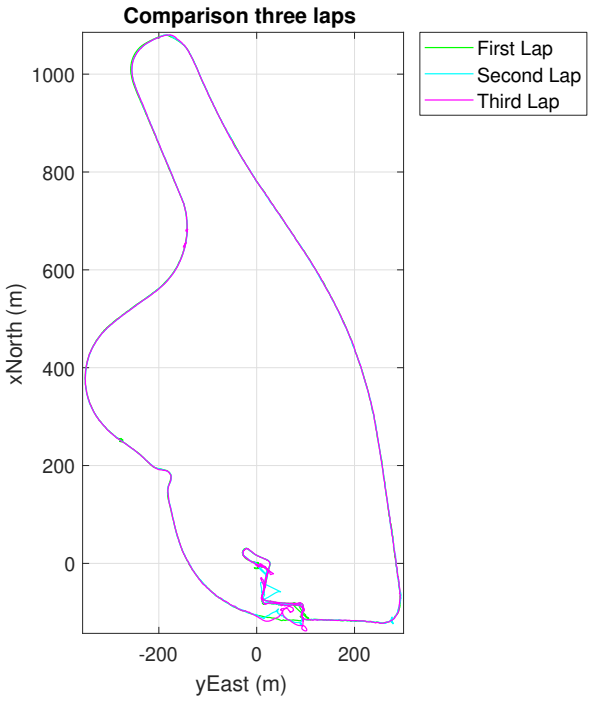

Figure 16: Comparison between the three laps.

It can be concluded that there is consistency in most of the test except for the start/end section of the circuit, Figure 17.

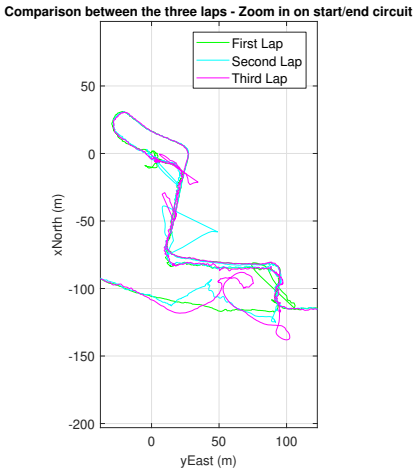

Figure 17: Comparison between the three circuits - zoom in on start/end circuit.

From data analysis it was found that lap 3 was the one with more GPS losses (4 flaws with a maximum flaw time, each, of 0.2s).

Lap 3 is shown in Figure 18. The red solution is the one with GPS aiding, and the blue one corresponds to the solution where there is no GPS.

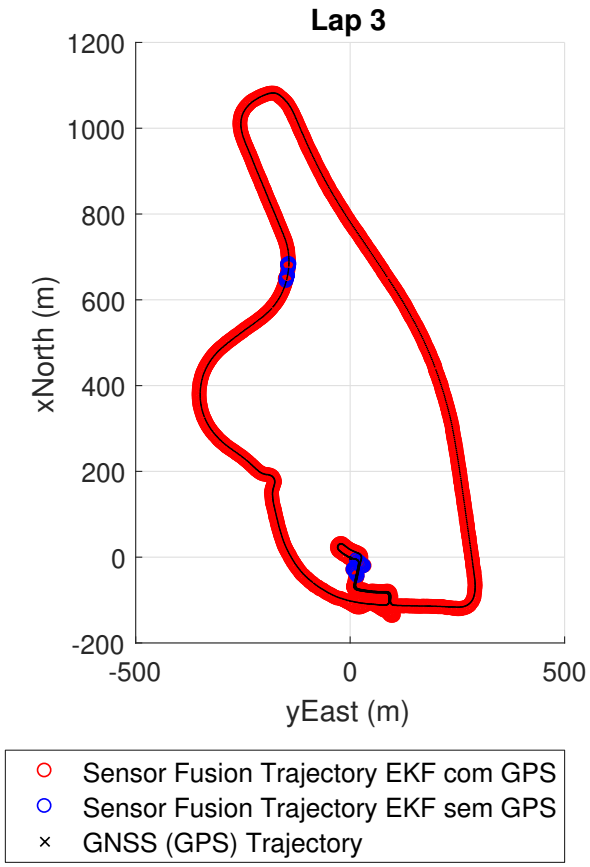

Figure 18: Lap 3.

Figures 19a and 19b represent the details when there is GPS signal loss. The deviations obtained in the position when the GPS fails are characteristic of a loosely coupled integration.

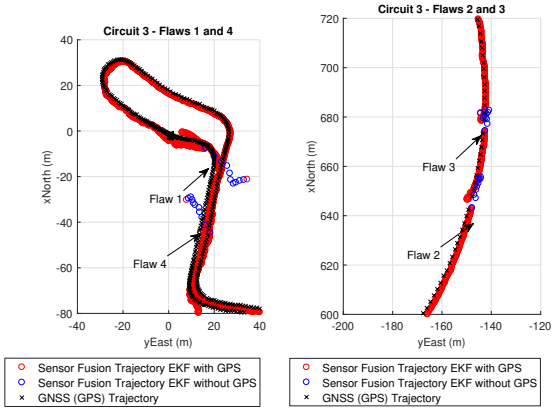

(a) Flaws 1 and 4. (b) Flaws 2 and 3.

Figure 19: Flaws lap 3.

A satellite photo, of the lap 3, is presented in Figure 20, which shows that the final solution on the horizontal plane is within road boundaries.

Figure 20: Satellite photo - lap 3.

In order to end the presentation of the results of the test in Figure 21, a graph is presented that shows the vertical profile of the whole test. The results presented show that there is consistency however, there is not precision on the altitude solution.

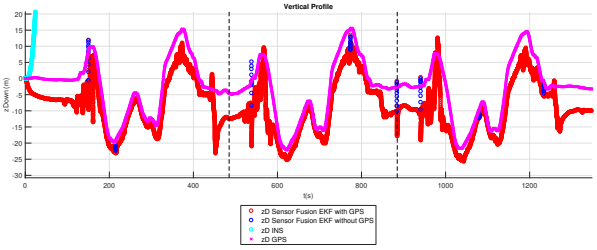

Figure 21: Vertical profile - real path - car.

5. Conclusions

In this paper a low cost navigation system was developed which aimed to be applied on an autonomous vehicle.

The implemented solution consists of the development of an EKF for GNSS/INS integration based on a GPS receiver and MEMS-based inertial sensors. The algorithm developed allows precise navigation solution, working at a sample frequency of 50Hz.

One of the main features of this study relates to the fact that the algorithm was developed without having any specific vehicle in mind. The aim was to develop an algorithm that would work not only in a dynamic outdoor environment but also in quasi-static indoor applications. Several tests were made in order to verify the operation of the system.

A simulator was developed in Simulink which allowed testing of the integration algorithm devel-

oped.

In a second phase the navigation system was implemented with real sensors. The developed system allows offline operation mode for post processing data and online operation mode for real time data processing.

From the simulation results presented it is possible to conclude that the system has good precision with or without GPS, especially on attitude estimation. In relation to position it is possible to have a high frequency and precise solution.

The yaw angle trial showed that the navigation system, operation in quasi-static indoor situations, can have a good estimate of the yaw angle. One of the important aspects learned from this test is that performing a good magnetometers calibration is extremely important.

The last test presented showed that vehicles' attitude was estimated with high precision. It was also possible to evaluate the consistency of the solution which was considered to be very good. There were not too many GPS signal losses, a fact that led to the conclusion that the receiver and the GPS antenna selected, despite being inexpensive, show good performance in an urban environment. The deviations obtained in the navigation solution are characteristic of the kind of integration implemented.

References

[1] P. Aggarwal, Z. Syed, A. Noureldin, and N. El-Sheimy. *MEMS-Based Integrated Navigation.* Artech House, 2010.

[2] J. D. Barton. Fundamentals of Small Unmanned Aircraft Flight. *Johns Hopkins Apl Technical Digest*, 31(2):132–149, 2012.

[3] G. Cai, T. H. Lee, and B. M. Chen. *Unmanned Rotorcraft Systems.* Springer-Verlag London Limited, 2011. (1st ed.).

[4] C. Cappelle, D. Pomorski, and Y. Yang. GPS/INS Data Fusion for Land Vehicle Localization. *The Proceedings of the Multiconference on Computational Engineering in Systems Applications*, 2:21–27, 2006.

[5] H. Cheng. *Autonomous Intelligent Vehicles - Theory, Algorithms, and Implementation.* Springer, 2011. (2nd ed.).

[6] N. El-Sheimy, E.-H. Shin, and X. Niu. Kalman Filter Face-Off: Extended vs Unscented Kalman Filters for Integrated GPS and MEMS Inertial. *Inside GNSS*, pages 48–54, 2006.

[7] P. Groves. *Principles of GNSS, Inertial, and Multisensor Integrated Navigation Systems*, volume 53. Artech House, 2008. (1st ed.).

[8] M. G. Petovello, M. E. Cannon, and G. Lachapelle. Development and Testing of a Real-Time GPS / INS Reference System for Autonomous Automobile Navigation. *Technology*, (August 2015):1–8, 2001.

[9] D. Titterton and J. L. Weston. *Strapdown inertial navigation technology. - 2nd ed.* The Institution of Electrical Engineers, 2004. (2nd ed.).

[10] O. J. Woodman. An Introduction to Inertial Navigation. *University of Cambridge*, (696):1–37, 2007.

A. Navigation EKF Equations

$$\frac{\mathrm{d}\boldsymbol{x}}{\mathrm{d}t} = \begin{bmatrix} \begin{bmatrix} \dot{\phi} \\ \dot{\theta} \\ \dot{\psi} \end{bmatrix} \\ \begin{bmatrix} \dot{P_{x_n}} \\ \dot{P_{y_n}} \\ \dot{P_{z_n}} \\ \dot{V_{x_n}} \\ \dot{V_{y_n}} \\ \dot{V_{z_n}} \end{bmatrix} \end{bmatrix} = \begin{bmatrix} \begin{bmatrix} 1 & \sin\phi\tan\theta & \cos\phi\tan\theta \\ 0 & \cos\phi & -\sin\phi \\ 0 & \dfrac{\sin\phi}{\cos\theta} & \dfrac{\cos\phi}{\cos\theta} \end{bmatrix} \begin{bmatrix} \omega_{x_{gyro}} \\ \omega_{y_{gyro}} \\ \omega_{z_{gyro}} \end{bmatrix} \\ \begin{bmatrix} V_{x_n} \\ V_{y_n} \\ -V_{z_n} \end{bmatrix} \\ C_b^n \begin{bmatrix} f_{x_{accel}} \\ f_{y_{accel}} \\ f_{z_{accel}} \end{bmatrix} + \begin{bmatrix} 0 \\ 0 \\ g \end{bmatrix} \end{bmatrix} \tag{A.5}$$

$$\boldsymbol{z} = \begin{bmatrix} \begin{bmatrix} m_{x_{mag}} \\ m_{y_{mag}} \\ m_{z_{mag}} \end{bmatrix} \\ \begin{bmatrix} P_{x_{nGPS}} \\ P_{y_{nGPS}} \\ P_{z_{nGPS}} \\ V_{x_{nGPS}} \\ V_{y_{nGPS}} \\ V_{z_{nGPS}} \end{bmatrix} \end{bmatrix} = \begin{bmatrix} C_n^b \begin{bmatrix} m_{x_n} \\ m_{y_n} \\ m_{z_n} \end{bmatrix} \\ \begin{bmatrix} P_{x_n} \\ P_{y_n} \\ P_{z_n} \\ V_{x_n} \\ V_{y_n} \\ V_{z_n} \end{bmatrix} \end{bmatrix} \tag{A.6}$$

$$\boldsymbol{z} = \begin{bmatrix} \begin{bmatrix} m_{x_{mag}} \\ m_{y_{mag}} \\ m_{z_{mag}} \end{bmatrix} \\ \begin{bmatrix} f_{x_{accel}} \\ f_{y_{accel}} \\ f_{z_{accel}} \end{bmatrix} \end{bmatrix} = \begin{bmatrix} C_n^b \begin{bmatrix} m_{x_n} \\ m_{y_n} \\ m_{z_n} \end{bmatrix} \\ \left(\begin{bmatrix} \omega_{x_{gyro}} \\ \omega_{y_{gyro}} \\ \omega_{z_{gyro}} \end{bmatrix} \times C_n^b \begin{bmatrix} V_{x_n} \\ V_{y_n} \\ V_{z_n} \end{bmatrix} \right) - g \begin{bmatrix} -\sin\theta \\ \sin\phi\cos\theta \\ \cos\phi\cos\theta \end{bmatrix} \end{bmatrix} \tag{A.7}$$